



# An approach to elucidating photocatalytic reaction mechanisms by monitoring dissolved oxygen: Effect of H<sub>2</sub>O<sub>2</sub> on photocatalysis

Tsutomu Hirakawa<sup>\*</sup>, Chifumi Koga, Nobuaki Negishi, Koji Takeuchi, Sadao Matsuzawa

National Institute of Advanced Industrial Science and Technology (AIST), Tsukuba-west 16-1, Onogawa, Tsukuba, Ibaraki 305-8569 Japan

## ARTICLE INFO

### Article history:

Received 16 April 2008

Received in revised form 14 August 2008

Accepted 21 August 2008

Available online 5 September 2008

### Keywords:

Photocatalyst

Ethanol

Oxygen

Hydrogen peroxide

## ABSTRACT

We present a method to analyze the photocatalytic oxidation of ethanol (EtOH) in an aqueous TiO<sub>2</sub> suspension by measuring the consumption of dissolved oxygen (DO) as a function of varying EtOH and H<sub>2</sub>O<sub>2</sub> concentrations in the suspension. The consumption of DO was analyzed by means of Langmuir–Hinshelwood (L–H) kinetics. The parameter  $K_{D-DO}$  calculated from L–H kinetics, defined as  $(O_2 \text{ consumption rate constant}) / (O_2 \text{ reproduction rate constant})^{-1}$ , reflects the adsorption equilibrium of EtOH and the photocatalytic reaction mechanisms. The observed  $K_{D-DO}$  values for the photocatalytic oxidation of EtOH reflected to the proposed reaction mechanism measured by HPLC and starch–iodine methods. By using this DO analysis method, we elucidated the photocatalytic reaction mechanism of EtOH oxidation and discussed the effect of H<sub>2</sub>O<sub>2</sub> as active oxygen species on TiO<sub>2</sub> photocatalysis.

© 2008 Elsevier B.V. All rights reserved.

## 1. Introduction

TiO<sub>2</sub> photocatalysis is a commonly used method for the decomposition and mineralization of environmental pollutants and other undesirable compounds [1]. Molecular oxygen (O<sub>2</sub>) is consumed in the reaction, and the O<sub>2</sub> consumption has been studied in the context of O<sub>2</sub> “photo-adsorption” and water splitting [2,3]. Studies of the role of O<sub>2</sub> have revealed that the reaction actually proceeds by the simultaneous reduction and oxidation of O<sub>2</sub> [4].

Oxygen has three important roles in photocatalysis [5–24]. First, the reduction of O<sub>2</sub> improves the photocatalytic activity to promote electron–hole (e<sup>−</sup>–h<sup>+</sup>) charge separation [5–7]. Second, O<sub>2</sub> accepts electrons generated in TiO<sub>2</sub> and is reduced to O<sub>2</sub><sup>•−</sup>, H<sub>2</sub>O<sub>2</sub>, OH radicals, and Ti–O<sup>•</sup> (or Ti–•OH). These surface-active species promote the photocatalytic oxidation of organic compounds [5–11]. Finally, upon oxidation, O<sub>2</sub> combines with organic radicals, which are generated by the reaction of holes with the reactant, to produce oxygen adduct intermediates such as organoperoxy radicals (ROO<sup>•</sup>) [12–24]. These intermediates are mineralized to CO<sub>2</sub> and H<sub>2</sub>O by consuming O<sub>2</sub>. Hence, O<sub>2</sub> is an indispensable molecule in photocatalytic reaction pathways, as represented in Scheme 1.

Thus far, the roles of O<sub>2</sub> in photocatalysis have been studied mainly by means of water splitting, ESR measurement for

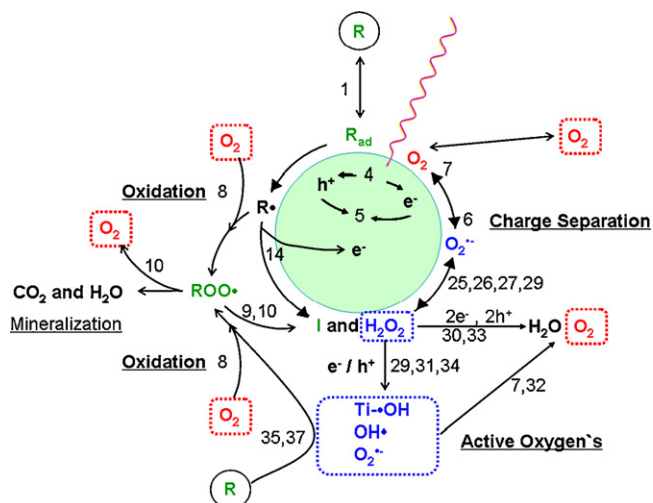
observing producing O<sub>2</sub><sup>•−</sup> and Ti<sup>3+</sup> disappearing and a decomposition of organic compounds as an effect of oxygen and by analysis of O<sub>2</sub> reduction processes on TiO<sub>2</sub>/polymer hybrid films [2,25–28]. A technique known as the chemical oxygen demand test, which is based on measuring oxygen consumption in TiO<sub>2</sub> photocatalysis, has recently been developed to estimate water pollution [29,30]. On the other hands, we reported at first time the utilization of O<sub>2</sub> to estimate photocatalytic activity by analyzing the oxygen decay process [31]. In the estimation, ethanol (EtOH) and iso-propanol (i-PrOH) are employed as standard compounds because these alcohols are completely decomposed to CO<sub>2</sub> and H<sub>2</sub>O through a well-studied, oxygen-assisted photocatalytic mineralization [11–24].

Many intermediate species are produced in the photocatalytic reaction process, including oxygenated intermediates that may be further oxidized to H<sub>2</sub>O and CO<sub>2</sub> [11–21]. Large amounts of O<sub>2</sub><sup>•−</sup> and H<sub>2</sub>O<sub>2</sub> are also produced in TiO<sub>2</sub> photocatalysis, and the generated H<sub>2</sub>O<sub>2</sub> is reduced and oxidized to OH radicals and O<sub>2</sub><sup>•−</sup>. In this way, H<sub>2</sub>O<sub>2</sub> is decomposed to H<sub>2</sub>O and O<sub>2</sub> through organic compound mineralization [5–10,21]. Therefore, we can assume that H<sub>2</sub>O<sub>2</sub> is one of the intermediate from the viewpoint of O<sub>2</sub> in the TiO<sub>2</sub>-photocatalyzed mineralization of organic compounds. Reactions involving H<sub>2</sub>O<sub>2</sub> are also represented in Scheme 1.

Since O<sub>2</sub> consumption and CO<sub>2</sub> production occur simultaneously in TiO<sub>2</sub>-photocatalyzed decomposition of organic compounds, we strongly suspected that the decomposition mechanism for TiO<sub>2</sub> photocatalysis could be elucidated by monitoring the behavior of O<sub>2</sub>. However, such a study had never been carried out.

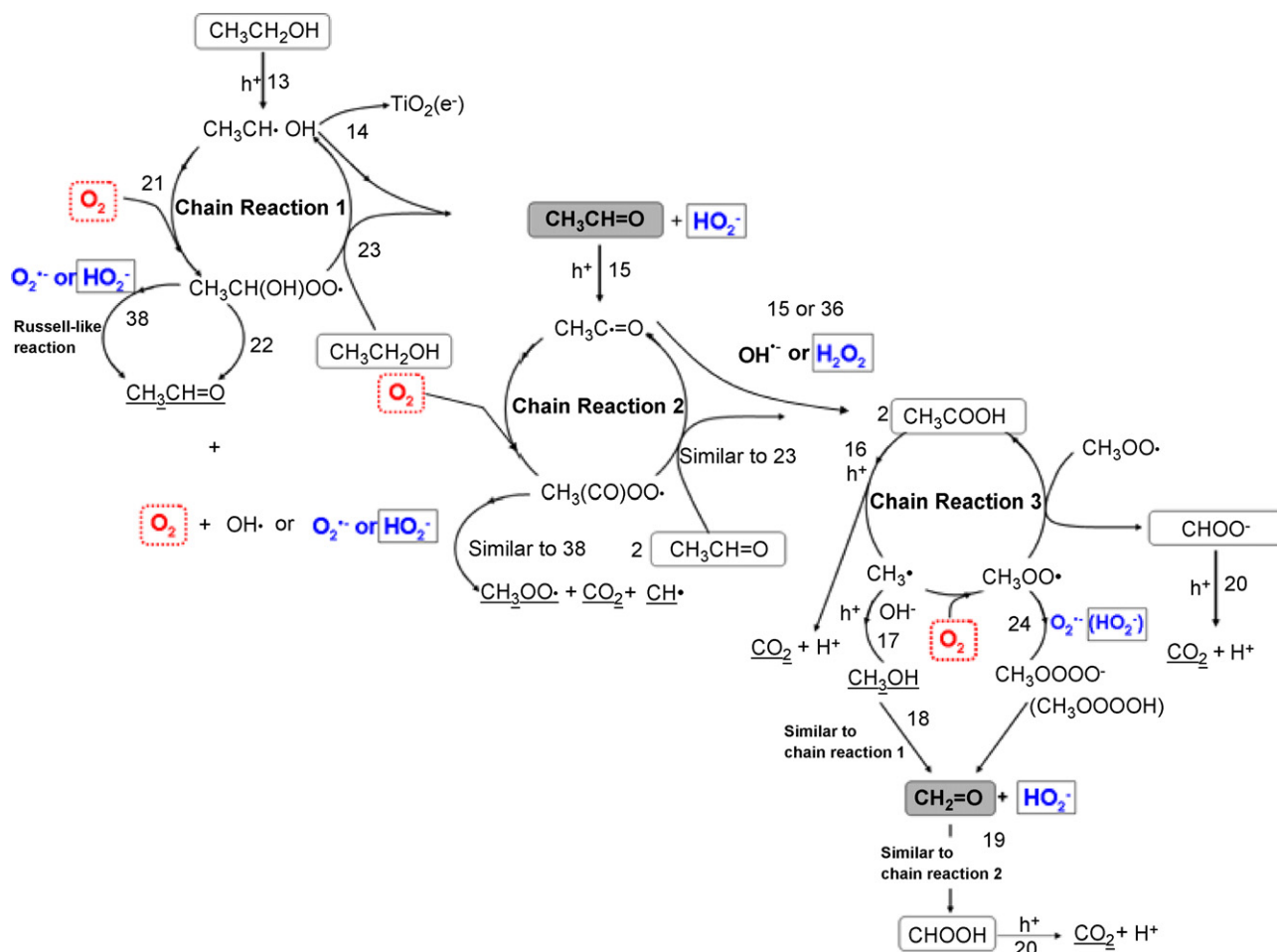
<sup>\*</sup> Corresponding author. Tel.: +81 29 861 8051; fax: +81 29 861 8866.

E-mail address: [t-hirakawa@aist.go.jp](mailto:t-hirakawa@aist.go.jp) (T. Hirakawa).



**Scheme 1.** Photocatalytic reaction mechanism for O<sub>2</sub>-assisted decomposition of organic compounds at TiO<sub>2</sub>\*. R, R<sub>ad</sub> and ROO\* are the organic reactant, adsorbed reactant and oxygenated reactant intermediate, respectively.

In the present study, we attempt to quantitatively and kinetically analyze EtOH oxidation in a TiO<sub>2</sub> photocatalytic system by monitoring both behavior of dissolved oxygen (DO) and H<sub>2</sub>O<sub>2</sub>. We used EtOH as the model organic compound in the present study because its reaction mechanism has been widely studied, as represented in Scheme 2 [12–19].



**Scheme 2.** Photocatalytic reaction mechanism for O<sub>2</sub>-assisted ethanol decomposition. CH<sub>3</sub>C=O, CH<sub>2</sub>=O, H<sub>2</sub>O<sub>2</sub>, O<sub>2</sub><sup>•-</sup>, and O<sub>2</sub> were measured in this study.

## 2. Experimental

### 2.1. Materials

TiO<sub>2</sub> powder (P25, Nippon aerogel) was used as a photocatalyst. A thin layer of P25 TiO<sub>2</sub> was placed on glass and exposed to UV light (SANKYO DENKI BLB Hg Lamp) at 354 nm for 120 h under ambient to completely decompose any surface pollutants. The UV-treated P25 powder was stored in a glass bottle in the dark. The complete decomposition of surface pollutants was estimated by stopping dissolved oxygen (DO) consumption in suspension [31,32]. Distilled water for HPLC (Wako) was used to prepare an TiO<sub>2</sub> suspension. Ethanol (Wako, 99.5%), acetaldehyde (Wako, 95%) and formaldehyde (SIGMA, 37%; contains 10–15% methanol) were used without further purification.

### 2.2. Analytical methods

#### 2.2.1. Monitoring consumption of dissolved oxygen

The behavior of DO during photocatalysis of the TiO<sub>2</sub> suspension was monitored with electrode for DO sensor (UC-12-SOL, Central Kagaku Co.), which was connected to a computer. A 100 mL colorimetric bottle (As-one) was used to effectively irradiate the TiO<sub>2</sub> suspension with UV light.

For DO monitoring, a TiO<sub>2</sub> suspension was prepared in 100 mL of 0.01 M NaOH, and the suspension was agitated by ultrasonic for 10 min. After agitation, the suspension was transferred to the colorimetric bottle and a known concentration of EtOH was added,

and was stirred vigorously for 30 min under ambient to establish DO equilibrium within the suspension. The electrode for DO sensor was then immersed in the suspension, and the bottle was sealed with a Teflon or silicon cap. The suspension filled the bottle completely so that there was no space for air in the system. The suspension was stirred vigorously during experiments. UV irradiation was carried out with four black light bulbs (FL10B, Toshiba). The light intensity was measured with a photometer (UV Caremate Pro, Fuji Xerox) and was  $2.7 \text{ mW cm}^{-2}$  inside the bottle. The temperature of the suspension was maintained at 295 K by directing a fan toward the bottle to prevent temperature increases. Other details for these DO measurements have been described elsewhere [31].

### 2.2.2. Analysis of acetaldehyde and formaldehyde

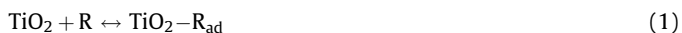
The acetaldehyde and formaldehyde generated from photocatalysis with EtOH were measured by HPLC (Shimadzu LC-10AT) equipped with a photodiode array detector (Shimadzu) [33]. Experimental concentrations of acetaldehyde and formaldehyde were estimated by fitting experimental data to calibration curves of known acetaldehyde and formaldehyde concentrations. After photocatalysis, the  $\text{TiO}_2$  suspension was filtered through a  $0.2 \mu\text{m}$  polypropylene disposable filter (Whatman), and the pH of the supernatant was adjusted to 2 with  $1 \text{ M HNO}_3$ . The supernatant was added to acetonitrile containing 2,4-dinitrophenylhydrazine (2,4-DNPH) to form the 2,4-DNPH derivatives of the aldehydes.

### 2.2.3. Analysis of $\text{H}_2\text{O}_2$

The amount of  $\text{H}_2\text{O}_2$  photocatalytically produced was estimated by the starch–iodine method. Before the addition of  $\text{I}^-$  and starch, the  $\text{TiO}_2$  suspension was filtered and the supernatant pH was adjusted as described in Section 2.2.2. After addition of  $\text{I}^-$  and starch, the solution was kept in the dark for 5 min in order to finish the reaction. The absorption at  $\text{I}^{3-}$  was measured with the UV–vis–NIR spectrometer (UV-3600 Shimadzu). The experimental concentration of  $\text{H}_2\text{O}_2$  was estimated by fitting the experimental data to a calibration curve constructed from known concentrations of  $\text{H}_2\text{O}_2$ .

### 2.3. The parameter obtained from L–H kinetics for DO consumption

In Langmuir–Hinshelwood (L–H) kinetics, the maximum DO consumption rate ( $r_{\text{max}}$ ) and the equilibrium constant ( $K_D$ ) for the adsorption reaction



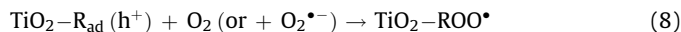
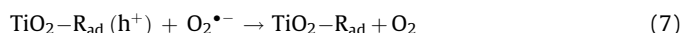
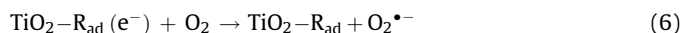
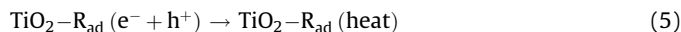
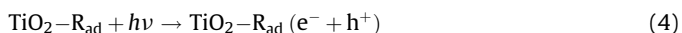
are calculated by plotting the inverse of the DO decay rate ( $r_{\text{DO}}$ ) against the inverse of the reactant concentration  $[\text{R}]$ :

$$\frac{1}{r_{\text{DO}}} = \frac{1}{r_{\text{max}}} + \frac{1}{r_{\text{max}}K_D[\text{R}]} \quad (2)$$

When the adsorption sites are fully occupied by reactant molecules,  $r_{\text{max}}$  is equivalent to  $r_{\text{DO}}$ . The other details of the  $r_{\text{max}}$  and L–H kinetics for DO consumption are described in our previous report [31]. The equilibrium constant  $K_D$  is given by the ratio of the rate constants for adsorption and desorption of reactant R at the  $\text{TiO}_2$  surface,  $K_D = k_1k_{-1}^{-1}$ , or

$$K_D = \frac{[\text{TiO}_2\text{--R}_{\text{ad}}]}{[\text{TiO}_2] \times [\text{R}]} \quad (3)$$

In  $\text{TiO}_2$  photocatalysis, the reactant adsorbed at the  $\text{TiO}_2$  surface ( $\text{R}_{\text{ad}}$ ) is oxidized to other intermediates and  $\text{CO}_2$  by consuming and reproducing  $\text{O}_2$ , as shown in the following equations:



In these equations,  $\text{ROO}^{\bullet}$  and I represent intermediates and oxygenated radical intermediates. We assumed that the  $K_D$  values observed in this study reflected both the adsorption and desorption of  $\text{O}_2$  [31]. Therefore,  $K_D$  for  $\text{O}_2$  consumption in our  $\text{TiO}_2$  photocatalysis can be defined as the reaction equilibrium for the consumption and reproduction of  $\text{O}_2$  ( $K_{D\text{-DO}}$ ), as shown in the following equation:

$$K_{D\text{-DO}} = [\text{TiO}_2\text{--R}_{\text{ad}}\text{--O}_2] ([\text{TiO}_2\text{--R}_{\text{ad}}][\text{O}_2])^{-1} \quad (11)$$

$K_{D\text{-DO}}$  is also represented by Eq. (12), which demonstrates the adsorption equilibrium of R and the photocatalytic reaction mechanism through rates of  $\text{O}_2$  consumption and reproduction [31]:

$$K_{D\text{-DO}} = (\text{O}_2 \text{ consumption rate constant}) / (\text{O}_2 \text{ reproduction rate constant})^{-1} \quad (12)$$

Since a large  $K_{D\text{-DO}}$  value is attributable to the irreversible reaction to consume DO, a large observed  $K_{D\text{-DO}}$  should indicate more efficient photocatalytic mineralization. According to the definition of the reaction (12), varying  $K_{D\text{-DO}}$  values reflect a proceeding the varying photocatalytic reaction.

## 3. Results

### 3.1. Dependency of ethanol concentration on DO consumption

Fig. 1 shows DO decay during the photocatalytic oxidation of varying concentrations of EtOH. The DO decay rate,  $r_{\text{DO}}$ , increased with increasing concentrations of EtOH. When the EtOH concentration was 5 mM, the DO was completely consumed within 20 min of UV irradiation. The DO decay process obeyed zero-order reaction kinetics (i.e., the decay rate was constant), indicating that the DO consumption in this experimental condition was a light intensity limiting reaction [31].

In Fig. 2(a),  $r_{\text{DO}}$  was plotted as a function of EtOH concentration and was apparently obeyed isothermal lines. However, because the reciprocal plot had two steps near 5 mM of EtOH as shown in Fig. 2(b), the data could not be analyzed by simple L–H kinetics. Instead, the data were divided into low (<5 mM) and high (>5 mM) EtOH concentration ranges, and each of the two ranges was independently fitted by Eq. (2), as shown in Fig. 3. Values of  $r_{\text{max}}$  and  $K_{D\text{-DO}}$  were then calculated from the plots in Fig. 3. The  $r_{\text{max}}$  and  $K_{D\text{-DO}}$  obtained were  $11.9 \mu\text{M min}^{-1}$  and  $5610 \text{ M}^{-1}$ , respectively, in the low EtOH concentration range and  $21 \mu\text{M min}^{-1}$  and  $452 \text{ M}^{-1}$ , respectively, in the high EtOH concentration range. These calculated parameters were used to fit the data shown in the inset of Fig. 2(a), and the resulting fits suggest that the data obeyed L–H kinetics for all EtOH concentrations studied. These results indicate that the reaction mechanism is changed at each concentration range of EtOH.

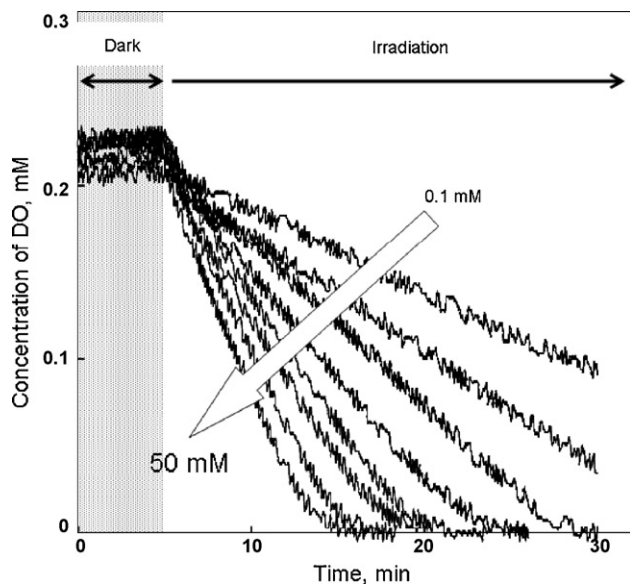


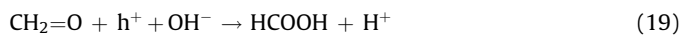
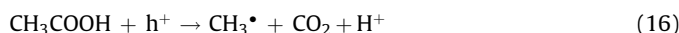
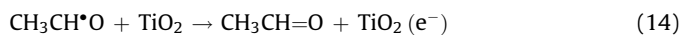
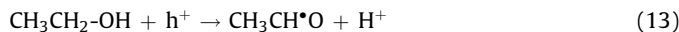
**Fig. 1.** DO consumption during  $\text{TiO}_2$  photocatalysis in an aqueous suspension containing EtOH at concentrations between 0.1 and 50 mM.  $\text{TiO}_2$  powder (P25,  $0.1 \text{ g L}^{-1}$ ) was suspended in 0.01 M NaOH (pH 11.5) and stirred in the dark for 5 min prior to UV irradiation.

### 3.2. Production of acetaldehyde and formaldehyde as intermediates

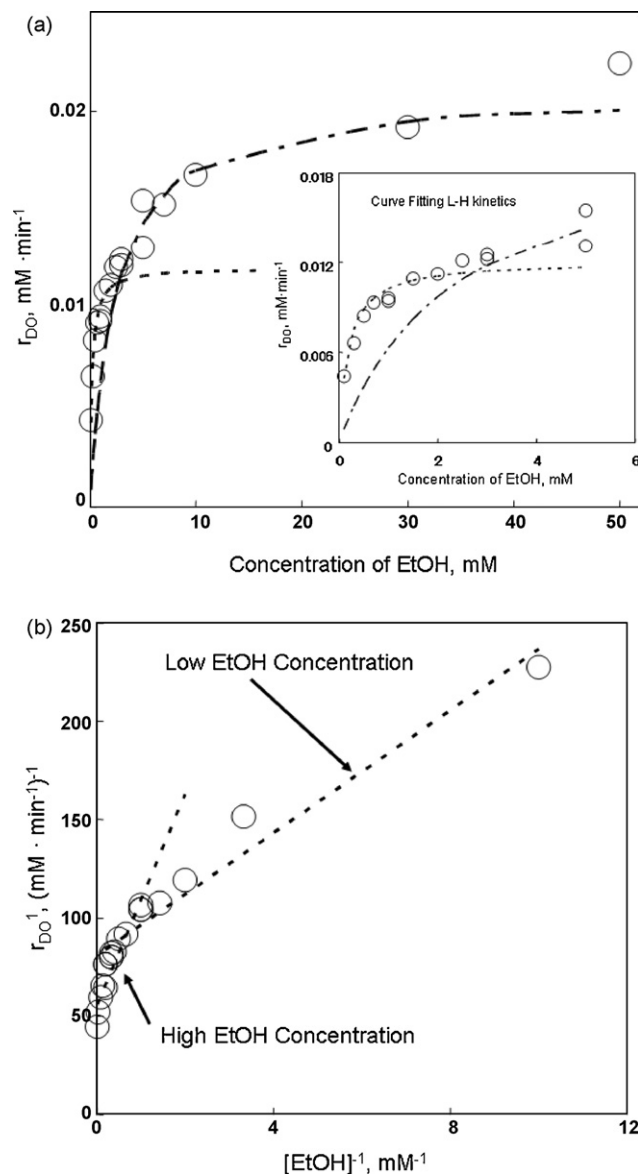
As stated above, the DO consumption during photocatalysis varied with EtOH concentration. Therefore, we expected that the amounts of major intermediate molecules produced from EtOH oxidation, such as acetaldehyde and formaldehyde, also varied with EtOH concentration as represented in Scheme 2 [34]. To verify this hypothesis, we measured the acetaldehyde and formaldehyde generated during photocatalysis. The UV-irradiation was ceased at 25 min or when DO was completely consumed.

Fig. 4 shows the concentrations of acetaldehyde ( $\diamond$ ) and formaldehyde ( $\circ$ ) produced as a function of EtOH concentration. The concentration of acetaldehyde increased with increasing EtOH concentration, with the rate of increase slowing substantially at concentrations higher than 1 mM. By contrast, the concentration of generated formaldehyde reached a maximum at 1 mM EtOH and decreased above this EtOH concentration.

The proposed mechanism for photocatalytic oxidation of EtOH is shown in the following equations [11–19]:



As shown by these equations, both acetaldehyde and formaldehyde are produced through the photocatalytic oxidation of EtOH. The observed decrease in formaldehyde at EtOH concentrations above 1 mM might be explained by considering that Eq. (15)



**Fig. 2.** (a)  $r_{\text{DO}}$  plotted as a function of EtOH concentration. Inset shows curve fitting using  $r_{\text{max}}$  and  $K_{\text{D-DO}}$  values obtained from L-H analysis of the data (shown in Fig. 3(a)). (b)  $1/r_{\text{DO}}$  plotted as a function of  $[\text{EtOH}]^{-1}$ .

are inhibited by the Eqs. (13) and (14), indicating that the photocatalytic reaction mechanism varied with EtOH concentration, as described in Section 3.1.

### 3.3. $\text{H}_2\text{O}_2$ production

In  $\text{TiO}_2$  photocatalysis of EtOH,  $\text{H}_2\text{O}_2$  is one of the intermediate molecules, indicating that  $\text{H}_2\text{O}_2$  strongly affects the photocatalytic reaction. To verify the dependence of these parameters upon  $\text{H}_2\text{O}_2$  concentration, we measured the production of  $\text{H}_2\text{O}_2$  during photocatalytic oxidation of varying concentrations of EtOH. The UV-irradiation was ceased at 25 min or when DO was completely consumed.

Fig. 5 shows the concentration of  $\text{H}_2\text{O}_2$  produced as a function of EtOH concentration. The absorbance at 360 nm attributable to  $\text{I}^{3-}$  could not be recognized above 5 mM EtOH because of the broad absorption. It might be attributable to products formed by interfering with the reaction of  $\text{H}_2\text{O}_2$ , starch, and  $\text{I}^-$  to produce



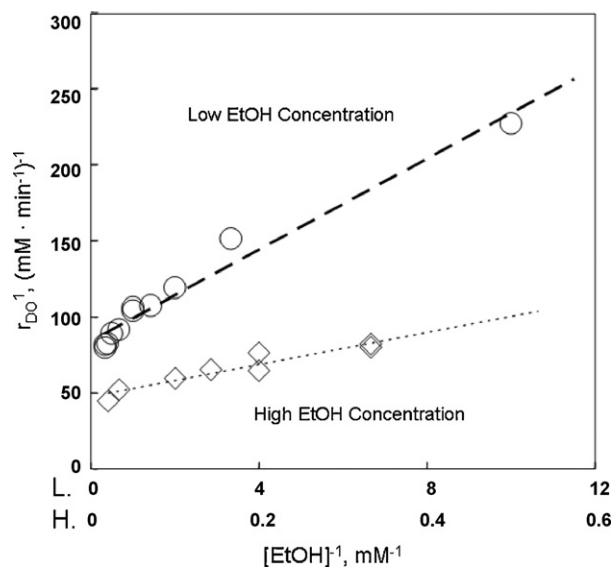


Fig. 3.  $1/r_{DO}$  plotted as a function of  $1/[EtOH]$ , in which the EtOH concentrations were separated into low (<5 mM) and high (>5 mM) ranges and subjected to L–H analysis.

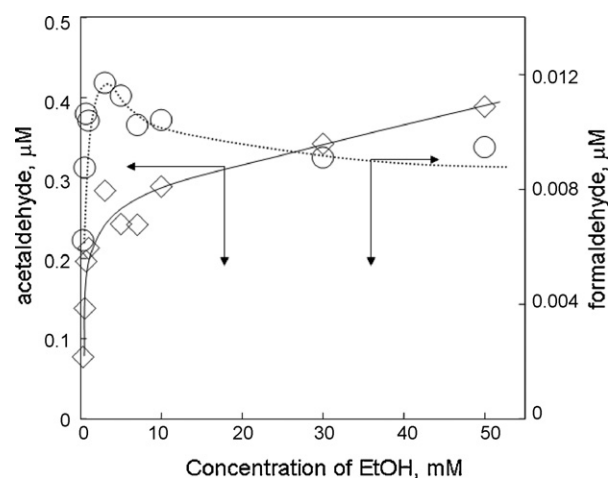


Fig. 4. Concentrations of acetaldehyde ( $\diamond$ ) and formaldehyde ( $\circ$ ) produced from the photocatalytic oxidation of EtOH at varying concentrations.

$I^{3-}$  with EtOH and an intermediates [35]. The concentration of  $H_2O_2$  produced was much higher than that of acetaldehyde or formaldehyde (Fig. 4). The  $H_2O_2$  concentration increased with increasing EtOH concentration, reaching a maximum of  $5 \mu M$   $H_2O_2$  at 1 mM EtOH. In the present study, since every experiment was carried out in closed system, the production of  $H_2O_2$  was stopped when all DO was consumed. Notably, no  $H_2O_2$  was detected in the absence of EtOH by the starch–iodine method.

$H_2O_2$  is produced from the equations below [36]:

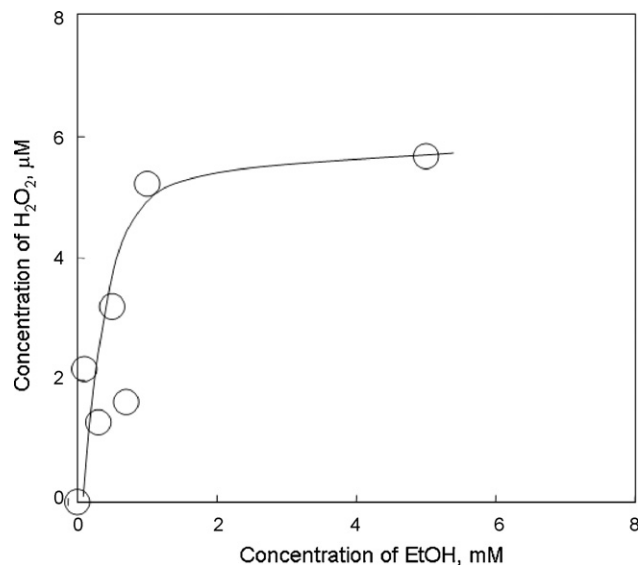
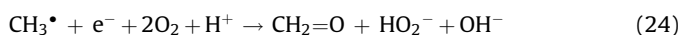
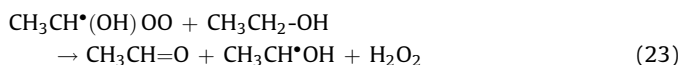
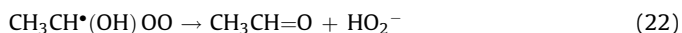
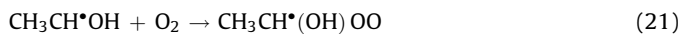
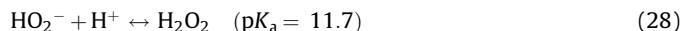
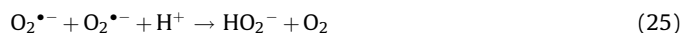


Fig. 5. Concentration of  $H_2O_2$  produced from the photocatalytic oxidation of EtOH at varying concentrations.

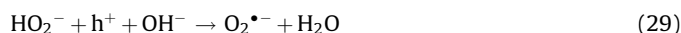


Eqs. (21)–(23) describe a well-known chain reaction for EtOH oxidation and subsequent acetaldehyde and  $H_2O_2$  production [13–15] and Eq. (24) is also suggested as production route through Eq. (16). Since the chain reaction is accelerated by the progress of the photocatalytic oxidation of EtOH (Eqs. (13)–(20)) as represented in Scheme 2, which inhibits charge recombination (Eq. (5)), the reaction in Eq. (6) is accelerated and large amounts of  $H_2O_2$  are produced through the reactions in Eqs. (25)–(27) [37–42].

### 3.4. Effect of $H_2O_2$ addition on $r_{DO}$ and $K_{D-DO}$

As seen in Fig. 5, a large amount of  $H_2O_2$  was produced by  $TiO_2$  photocatalysis with EtOH. However, determining the specific effect of  $H_2O_2$  on the photocatalysis process was difficult. To determine the effects of  $H_2O_2$  on the EtOH oxidation and DO consumption, we estimated  $r_{DO}$  and  $K_{D-DO}$  from photocatalysis reactions using varying known concentrations of  $H_2O_2$ .

Fig. 6 shows the DO decay for  $TiO_2$  photocatalysis with 0.1 mM of  $H_2O_2$  added to the  $TiO_2$  suspension. At low EtOH concentrations (Fig. 6(a)), an increase in the DO concentration was immediately observed upon UV irradiation of the suspension. This observation may reflect the production of  $O_2$  from  $H_2O_2$  oxidized by  $h^+$  (Eqs. (29), (30) and (7)) [5,7–9,37–43]:



This initial increase in DO upon UV irradiation diminished with increasing concentrations of EtOH, and at 7 mM EtOH, no initial increase was observed (Fig. 6(b)). Furthermore, the starting point for DO consumption was delayed by the addition of  $H_2O_2$  as seen in Fig. 7, suggesting the oxidation of EtOH by  $TiO_2$  photocatalysis

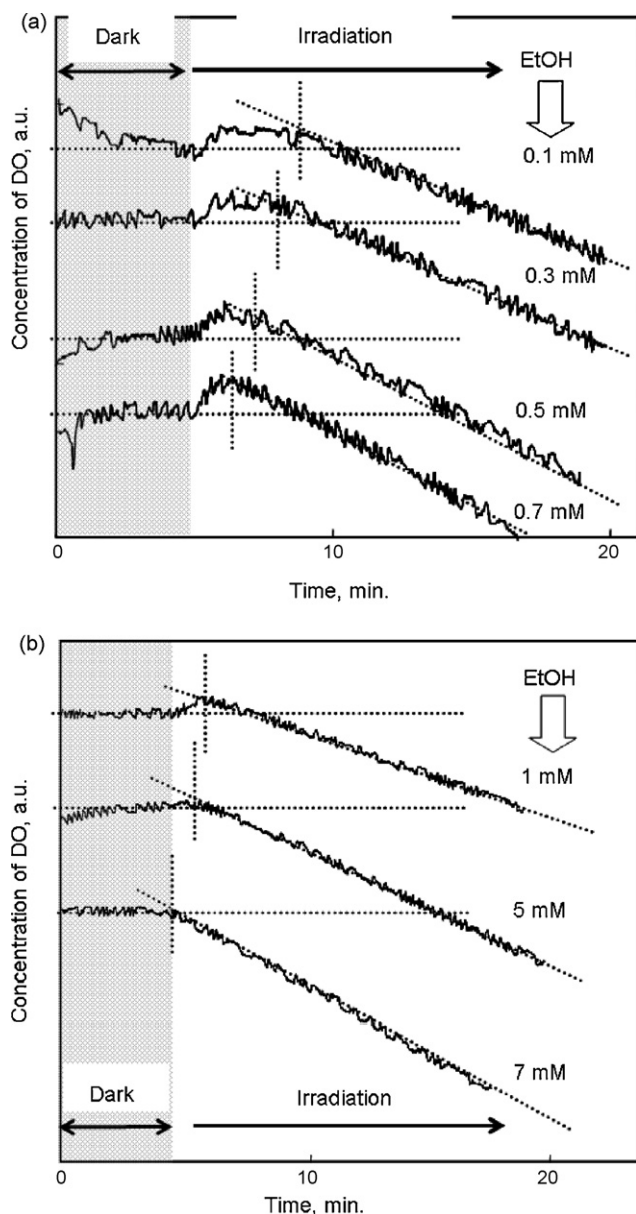


**Fig. 6.** DO concentration observed during photocatalysis of  $\text{TiO}_2$  suspensions containing 0.1 mM of previously added  $\text{H}_2\text{O}_2$  and several concentrations of EtOH: (a) 0.1–0.7 mM and (b) 1–7 mM.

(Eq. (13)) competed with oxidation of  $\text{H}_2\text{O}_2$  by  $h^+$  to produce  $\text{O}_2$  (Eqs. (29), (30) and (7)) [44].

The  $r_{\text{max}}$  of  $\text{H}_2\text{O}_2$  addition was also divided into two EtOH concentration ranges (not shown here), as described for Fig. 3, using 5 mM EtOH as a boundary point. Then,  $r_{\text{max}}$  and  $K_{\text{D-DO}}$  for L-H kinetics were calculated as  $9.7 \mu\text{M min}^{-1}$  and  $11,462 \text{ M}^{-1}$ , respectively, for the low EtOH concentration range and  $21 \mu\text{M min}^{-1}$  and  $428 \text{ M}^{-1}$ , respectively, for the high EtOH concentration range. The obtained  $r_{\text{max}}$  decreased upon addition of  $\text{H}_2\text{O}_2$  because the oxidation of  $\text{H}_2\text{O}_2$  (Eqs. (29), (30) and (7)) competed with EtOH oxidation (Eqs. (13–20)). Furthermore, the  $K_{\text{D-DO}}$  value for the low EtOH concentration range was increased by the addition of  $\text{H}_2\text{O}_2$ , indicating that the oxidation of EtOH by photocatalysis was accelerated and that an irreversible reaction resulting in the consumption of DO occurred. By contrast,  $r_{\text{max}}$  and  $K_{\text{D-DO}}$  for the high EtOH concentration range were the same as those obtained without added  $\text{H}_2\text{O}_2$ , suggesting that the contribu-

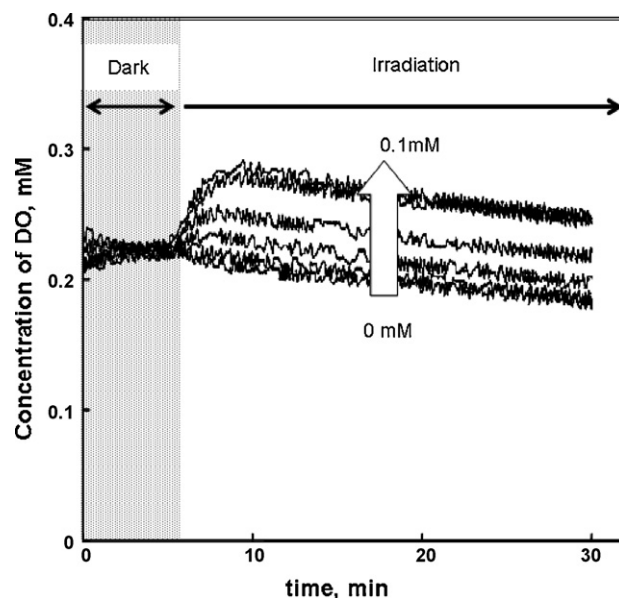


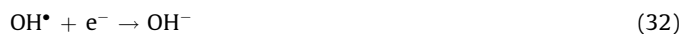
**Fig. 7.** DO concentration observed during photocatalysis of  $\text{TiO}_2$  suspensions containing 0.01–0.1 mM  $\text{H}_2\text{O}_2$ .

tion of  $\text{H}_2\text{O}_2$  toward photocatalytic EtOH oxidation might be negligibly small at high EtOH concentration.

Considering the above results, the reaction mechanism that contributed to  $\text{H}_2\text{O}_2$  production appears to differ for the two EtOH concentration ranges.

### 3.5. $\text{O}_2$ production by $\text{TiO}_2$ photocatalytic oxidation with $\text{H}_2\text{O}_2$

As stated above,  $\text{H}_2\text{O}_2$  contributed the oxidation of EtOH in the low EtOH concentration range. Therefore,  $\text{H}_2\text{O}_2$  is oxidized and reduced during photocatalysis as described in Eqs. (29), (30) and (7) as well as the reduction of  $\text{H}_2\text{O}_2$  to  $\text{H}_2\text{O}$  (Eqs. (31–33)) [5,7–9,37–43] and the ratio of progress for these two sets of reactions is 1:1 [45].



To verify this  $\text{H}_2\text{O}_2$  reaction ratio on photocatalysis, we measured the amount of DO produced from oxidation of  $\text{H}_2\text{O}_2$  in the absence of EtOH.

Fig. 7 shows the changes of DO concentration obtained when 0.01–0.1 mM  $\text{H}_2\text{O}_2$  was added before UV irradiation. The increase of DO concentration was observed immediately upon subjecting the suspension to UV irradiation and then the concentration of DO decayed slowly during the irradiation process. The  $r_{\text{DO}}$  value obtained from photocatalysis at each concentration of  $\text{H}_2\text{O}_2$  was almost the same as that obtained from photocatalysis without added  $\text{H}_2\text{O}_2$ .

Next, the increasing DO production rate in Fig. 7 was estimated, and the concentration of DO produced was calculated from the rate and plotted as a function of  $\text{H}_2\text{O}_2$  concentration, as shown in Fig. 8. The concentration of DO produced gently increased with increasing  $\text{H}_2\text{O}_2$  concentration. Though the concentration of DO was an averaged value, the DO consumption in the DO increment range was assumed to be negligible because  $r_{\text{DO}}$  is very small, as seen in Fig. 8. The  $\text{O}_2$  production ratio, defined as  $(\text{O}_2 \text{ production})/(\text{concentration of } \text{H}_2\text{O}_2 \text{ added})$ , is

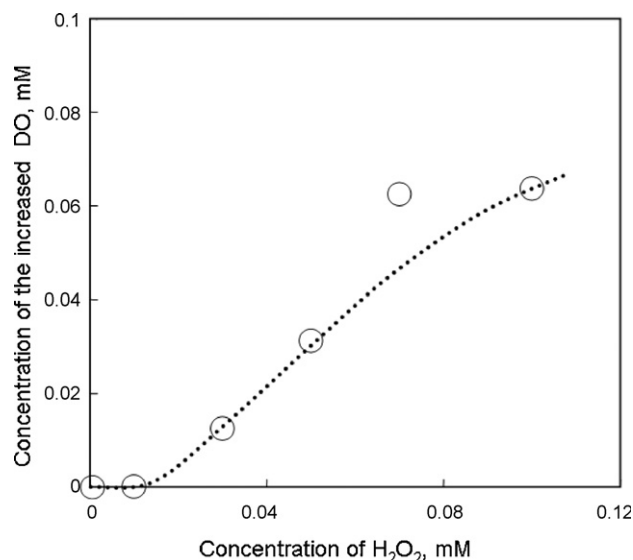


Fig. 8. DO concentration observed during photocatalysis of  $\text{TiO}_2$  suspensions containing 0.1 mM  $\text{H}_2\text{O}_2$  and no EtOH. The concentration was estimated from the increased rate of DO production observed in Fig. 7.

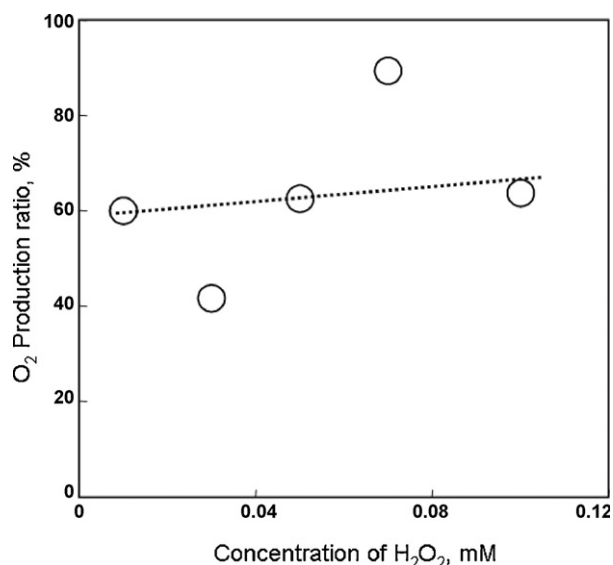


Fig. 9. Production ratios for  $\text{O}_2$  as a function of  $\text{H}_2\text{O}_2$  concentration.

shown in Fig. 9 for varying  $\text{H}_2\text{O}_2$  concentrations. We found that approximately 63% of the  $\text{H}_2\text{O}_2$  was oxidized to  $\text{O}_2$ , and we assumed that the remaining 37% was reduced to  $\text{H}_2\text{O}$ . The reduction ratio of  $\text{H}_2\text{O}_2$  was smaller than its oxidation ratio, indicating that reduction of  $\text{O}_2$  occurred.

## 4. Discussion

### 4.1. Relationship between $K_{D-DO}$ and the mechanism of the $\text{TiO}_2$ photocatalytic reaction

At the low EtOH concentration range,  $K_{D-DO}$  was large, and increasing concentrations of acetaldehyde and formaldehyde were observed. These results suggest that the oxidation of EtOH and acetaldehyde (Eqs. (13–20)) proceeded more readily with increasing concentrations of EtOH. By contrast, in the high EtOH concentration range,  $K_{D-DO}$  decreased to 0.1 times the value

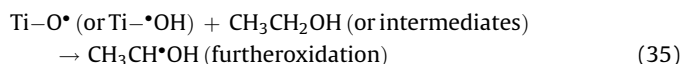
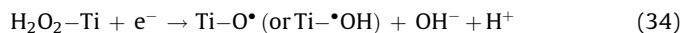
observed for the lower EtOH concentration range and the concentration of acetaldehyde increased, whereas that of formaldehyde decreased. Inhibition of the reaction (15) with increasing the concentration of EtOH indicates that the concentration of  $\text{CH}_3\text{COOH}$  at the surface and the production of  $\text{CO}_2$  are decreased. Hence the mineralization to consume DO become small and the  $K_{D-DO}$  decreased as mentioned in Section 3.1.

$\text{H}_2\text{O}_2$  was major produced as an intermediate during the photocatalytic oxidation of EtOH. Other groups have reported that  $\text{H}_2\text{O}_2$  is mainly produced from the photocatalytic oxidation of EtOH through Eqs. (21)–(23) [13]. The reaction rate constant associated with Eq. (23) is very slow ( $k = 10 \text{ M}^{-1} \text{ s}^{-1}$ ), indicating that the intermediate radical  $\text{CH}_3\text{CH}(\text{OH})\text{OO}^\bullet$  has to react with  $\text{CH}_3\text{CH}_2\text{-OH}$  before reacting at the surface of  $\text{TiO}_2$  to produce  $\text{CH}_3\text{CH=O}$  and  $\text{O}_2^{\bullet-}$  [13]. Considering this reaction pathway, the chain reaction proceeded more readily at high EtOH concentrations, whereas at low EtOH concentrations,  $\text{H}_2\text{O}_2$  production may occur through the reduction of  $\text{O}_2$  as depicted by Eqs. (25)–(27) and as stepwise carried out the reactions (21)–(23).

### 4.2. Effect of $\text{H}_2\text{O}_2$ addition on photocatalysis at low concentrations of EtOH

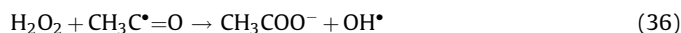
At low EtOH concentrations,  $K_{D-DO}$  increased upon the addition of  $\text{H}_2\text{O}_2$  to the  $\text{TiO}_2$  suspension, indicating that the photocatalytic oxidation of EtOH was accelerated by  $\text{H}_2\text{O}_2$ .

As shown in Fig. 6, an increase in DO was observed for EtOH concentrations of 0.1–7 mM, and the DO production kept on each period time for several minutes. If 0.1 mM  $\text{H}_2\text{O}_2$  was completely oxidized to  $\text{O}_2$  at each EtOH concentration, then the starting time for the decay of DO production should be delayed by increasing the concentration of EtOH. However, the observed delay shortened with increasing EtOH concentrations, indicating that the oxidation of intermediates was carried out more readily than the oxidation of  $\text{H}_2\text{O}_2$  to  $\text{O}_2$ . Furthermore, a slight decrement of  $r_{\text{max}}$  was observed when  $\text{H}_2\text{O}_2$  was added to the  $\text{TiO}_2$  suspension at lower EtOH concentrations. Since  $r_{\text{max}}$  was defined as the total of the  $\text{O}_2$  consumption and reproduction rates constant [31],  $\text{O}_2$  production from the oxidation of  $\text{H}_2\text{O}_2$  caused a decrease in  $r_{\text{max}}$ . However, the small difference between  $r_{\text{max}}$  values observed with and without  $\text{H}_2\text{O}_2$  also indicates that EtOH and intermediates was more readily oxidized than  $\text{H}_2\text{O}_2$ . Based on the suggestion, we can expect that the production of oxidative active species such as  $\text{HO}^\bullet$  (Eq. (31)),  $\text{Ti-O}^\bullet$ , and  $\text{Ti-OH}^\bullet$  (Eq. (34)) may be accelerated by accelerating the oxidation of EtOH (Eq. (35)):



Without addition of EtOH, the 63% of  $\text{H}_2\text{O}_2$  was oxidized to  $\text{O}_2$  as shown in Fig. 9. When the almost all of  $h^+$  photo-induced is reacted with EtOH and intermediate, the photocatalytic reduction of  $\text{H}_2\text{O}_2$  as Eqs. (31) to (33) is accelerated.

In addition, the reaction of  $\text{H}_2\text{O}_2$  and  $\text{CH}_3\text{C}^\bullet=\text{O}$  (Eq. (36)) may be also carried out, and this reaction is effective in the low EtOH concentration range:



Hence, we suggest that  $\text{H}_2\text{O}_2$  was effective to oxidize EtOH for increasing  $K_{D-DO}$  value in low EtOH concentration range.

#### 4.3. Effect of H<sub>2</sub>O<sub>2</sub> addition on photocatalysis at high concentrations of EtOH

At high EtOH concentrations,  $r_{\max}$  and  $K_{D-DO}$  were not changed by the addition of H<sub>2</sub>O<sub>2</sub>. These results can be explained by assuming that the amount of H<sub>2</sub>O<sub>2</sub> adsorbed at the surface decreased as the EtOH concentration increased. In fact, others have reported that H<sub>2</sub>O<sub>2</sub> and EtOH adsorb at Ti<sup>4+</sup> sites on the surface of TiO<sub>2</sub> [14,15,38,41,42,44,46]. Furthermore, since a high concentration of H<sub>2</sub>O<sub>2</sub> has been measured in the supernatant after removal of TiO<sub>2</sub> powder in previous TiO<sub>2</sub> photocatalysis studies using sacrificial reagents [38,39], H<sub>2</sub>O<sub>2</sub> may be not adsorbed at the surface or displaced by a sacrificial reagent and dispersed into the bulk solution because of the high concentration of EtOH and an intermediate than H<sub>2</sub>O<sub>2</sub>. Hence, we suggested that at high concentration of EtOH, the concentration of EtOH and intermediate adsorbed at the surface were higher than that of H<sub>2</sub>O<sub>2</sub>.

Notice here that H<sub>2</sub>O<sub>2</sub> might be reduced during TiO<sub>2</sub> photocatalysis even at high EtOH concentration. Since the conduction band e<sup>-</sup> is increased with oxidizing EtOH as have been known for current doubling effect [6,46], the photocatalysis with EtOH accelerates H<sub>2</sub>O<sub>2</sub> reduction to produce water as Eqs. (31)–(33). We assumed that the oxidation of H<sub>2</sub>O<sub>2</sub> as Eqs. (29) and (30) may be ruled out at high EtOH concentration region because the concentration of EtOH and an intermediate is much higher than that of H<sub>2</sub>O<sub>2</sub>. Hence, we suggested that the increase of adsorption of EtOH and an intermediate and the decrease of H<sub>2</sub>O<sub>2</sub> at the surface as the displacement may major reason for no positive effect of H<sub>2</sub>O<sub>2</sub> addition on photocatalytic oxidation of EtOH.

The production of HO• from H<sub>2</sub>O<sub>2</sub> via photolysis has also been reported [9]. However, under the present experimental conditions,  $r_{\max}$  and  $K_{D-DO}$  were not affected by the addition of H<sub>2</sub>O<sub>2</sub> at high EtOH concentrations, indicating that the photolysis of H<sub>2</sub>O<sub>2</sub> might be negligible at these concentrations and that Eqs. (34) and (35) might be the major reactions accelerating EtOH oxidation.

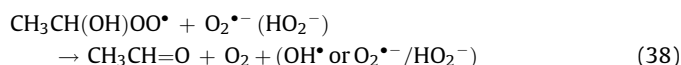
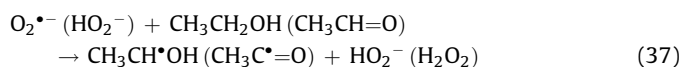
#### 4.4. Behavior of O<sub>2</sub> and H<sub>2</sub>O<sub>2</sub> produced from TiO<sub>2</sub> photocatalysis with EtOH

The production mechanism of H<sub>2</sub>O<sub>2</sub> is explained by considering Eqs. (25)–(27) as photocatalytic reduction of O<sub>2</sub>, and then O<sub>2</sub> firstly must be reduced to O<sub>2</sub><sup>•-</sup>. Oxygen molecules have been reported to

adsorb at Ti<sup>3+</sup> or Ti<sup>4+</sup> sites [25–27], suggesting that the steady-state amounts of O<sub>2</sub><sup>•-</sup> and O<sub>2</sub> decrease with increasing amounts of EtOH. On the basis of these suggestions, we expected that the behavior of O<sub>2</sub> and O<sub>2</sub><sup>•-</sup> in photocatalysis with EtOH was directly related to that of H<sub>2</sub>O<sub>2</sub> observed in this study [31].

For 0.1–1 mM EtOH, the H<sub>2</sub>O<sub>2</sub> was produced and the concentration increased as shown in Fig. 5. In fact, in our previous work in Ref. [28], the increase in the concentration of O<sub>2</sub><sup>•-</sup> was observed in the 0.1–1 mM of EtOH concentration range as a result of the acceleration of O<sub>2</sub> reduction [31]. Then Eqs. (25)–(27) might be accelerated to produce H<sub>2</sub>O<sub>2</sub>.

As shown in Fig. 5, for 1–5 mM EtOH, production of H<sub>2</sub>O<sub>2</sub> reached plateau. As have been shown in our previous work in Ref. [31], for 1–10 mM EtOH, the concentration of O<sub>2</sub><sup>•-</sup> decreased slowly, suggested that O<sub>2</sub><sup>•-</sup> might react with EtOH and intermediate as the chain reaction through Eqs. (37) and (38) known as Russell-like reactions [47] with competing with displacing from O<sub>2</sub>, O<sub>2</sub><sup>•-</sup> to EtOH and accelerating the reactions (25)–(27).

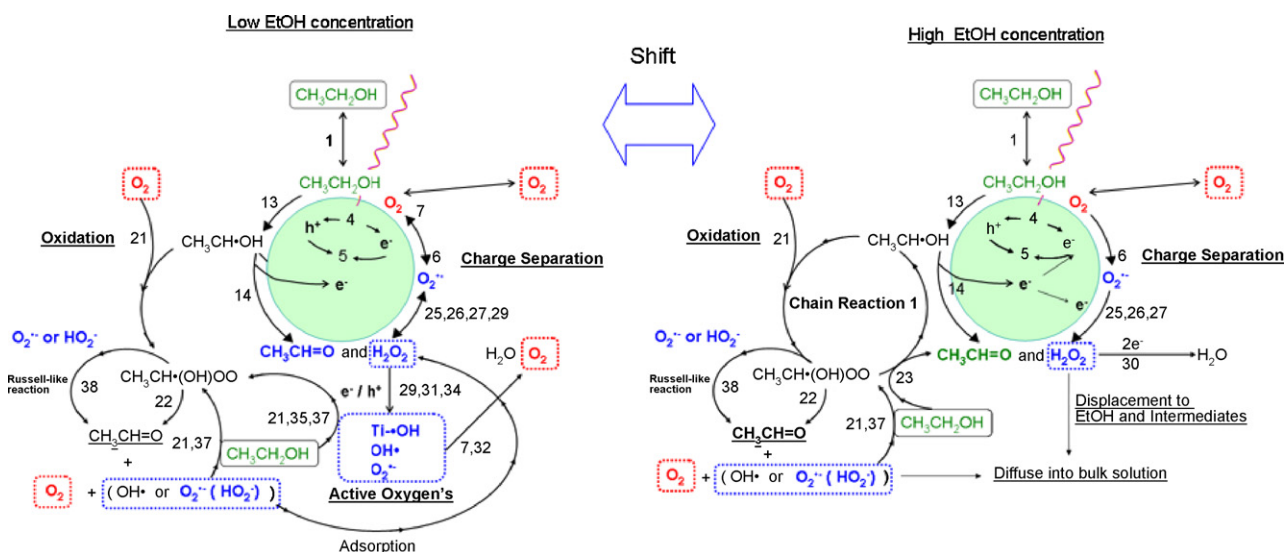


At higher EtOH concentrations than 10 mM, the concentration of O<sub>2</sub><sup>•-</sup> was significantly decreased in the previous work [31]. This result could be explained by considering the decreasing amount of O<sub>2</sub> adsorbed at the surface and the accelerating multi-reduction of O<sub>2</sub> to produce H<sub>2</sub>O (and/or Ti–OH) through Eqs. (31)–(33).

As stated above, the behavior of H<sub>2</sub>O<sub>2</sub> produced in TiO<sub>2</sub> photocatalysis with EtOH is consistent with the observation that the behavior of O<sub>2</sub><sup>•-</sup> produced in TiO<sub>2</sub> photocatalysis with EtOH [31]. The plausible reaction mechanism proposed in the present study is summarized in Scheme 3.

## 5. Summary

In the present study, we demonstrated that the mechanism of the photocatalytic reaction of EtOH can be analyzed by monitoring the O<sub>2</sub> and H<sub>2</sub>O<sub>2</sub> produced and consumed during the reaction. The consumption process of DO could be analyzed with



Scheme 3. Plausible reaction mechanism for EtOH decomposition at both low and high EtOH concentrations.



Langmuir–Hinshelwood kinetics. In the present study, the parameter  $K_{D-DO}$  calculated from L–H kinetics was defined as  $(O_2 \text{ consumption rate constant})/(O_2 \text{ reproduction rate constant})^{-1}$ , indicating that a large  $K_{D-DO}$  reflects a more irreversible  $O_2$  consumption with progressing photocatalytic oxidation of EtOH.

The  $K_{D-DO}$  value for the low EtOH concentration range (0.1–5 mM) was 10 times as high as the  $K_{D-DO}$  values observed for high EtOH concentrations (10–50 mM). Furthermore, by addition of 0.1 mM  $H_2O_2$ , the  $K_{D-DO}$  was increased in the low EtOH concentration range, whereas the addition of  $H_2O_2$  did not affect  $K_{D-DO}$  at high EtOH concentrations. In the results obtained from HPLC and starch–iodine methods to measure intermediates such as acetaldehyde, formaldehyde, and  $H_2O_2$ , production of larger amounts of acetaldehyde and  $H_2O_2$  were observed as the EtOH concentration increased, whereas the amount of formaldehyde decreased at high EtOH concentrations. These results indicate that further photocatalytic oxidation of acetaldehyde occurred in the lower ethanol concentration range, but that the reaction might cease at high EtOH concentrations till the concentration of acetaldehyde increased to higher than EtOH. Because the oxidation of acetaldehyde consumes large amounts of  $O_2$ , these results and the speculated reaction mechanism determined from the HPLC and I–starch methods supported the  $K_{D-DO}$  results obtained for the photocatalytic oxidation of EtOH and  $H_2O_2$ .

The detailed contribution of  $H_2O_2$  to  $TiO_2$  photocatalysis was also studied and appeared to be affected by the concentration of EtOH. In the low EtOH concentration range, oxidative radical species similar to  $OH^\bullet$ , such as  $Ti^\bullet-OH$  and  $Ti^\bullet-O^\bullet$ , that might be produced by photocatalytic reduction of  $H_2O_2$  appeared to be critical for the oxidation of EtOH. However, at high EtOH concentrations the contribution of  $H_2O_2$  was negligible, suggesting that increasing amounts of EtOH displaced the  $H_2O_2$  adsorbed at  $TiO_2$  surface and that a reduction of  $H_2O_2$  to produce  $H_2O$  might be accelerated. Because the oxidation EtOH intermediates may proceed more readily than that of  $H_2O_2$  to produce  $O_2$ , the reaction of reactants with  $O_2^{\bullet-}$  produced from the oxidation of  $H_2O_2$  may be ruled out.

In the absence of EtOH, approximately 63% of  $O_2$  and 37% of  $H_2O_2$  species are produced from photocatalytic reactions involving  $H_2O_2$ .  $H_2O_2$  reduction was relatively small because of the competing  $O_2$  reduction process.

As demonstrated in this study, this method permits the elucidation of photocatalysis reaction mechanisms by monitoring  $O_2$  and reactive oxygen species. This method is a powerful tool for obtaining information about photocatalytic reactions and could be applied in the treatment of wastewater.

## References

- [1] (a) M. Kaneko, I. Okura (Eds.), *Photocatalysis: Science and Technology*, Kodansha-Scientific, Tokyo, 2002, pp. P109–182; (b) A. Fujishima, T.N. Rao, D.A. Tryk, *J. Photochem. Photobiol. C: Photochem. Rev.* 1 (2000) 1; (c) A. Fujishima, K. Hashimoto, T. Watanabe, *Photocatalysis*, BKC Inc., Tokyo, 1999; (d) A. Mills, L.S. Hunte, *J. Photochem. Photobiol. A: Chem.* 108 (1997) 1.
- [2] (a) D.R. Kennedy, M. Ritchie, J. Mackenzie, *Trans. Farad. Soc.* 54 (1958) 119; (b) I.S. McIntock, M. Ritchie, *Trans. Farad. Soc.* 61 (1965) 1007; (c) R.I. Bickley, F.S. Stone, *J. Catal.* 31 (1973) 389; (d) V.S. Zakharenko, A.E. Charkashin, *React. Kinet. Catal. Lett.* 23 (1983) 131; (e) A.H. Boonstra, A.H.A.C. Mutsaers, *J. Phys. Chem.* 79 (1975) 1694.
- [3] (a) G. Munuera, J. Soria, J.C. Conesa, J. Sanz, A.R. Gonzalez-Elipe, E.J. Navio, A. Lopez-Molina, A. Muznoz, A. Fernandez, J.P. Espinos, *Catal. Energy Scene* 19 (1984) 335; (b) E. Borgarello, E. Pelizzetti, *Inorg. Chem. Acta* 91 (1984) 295.
- [4] (a) P. Salvador, C. Gutierrez, *Chem. Phys. Lett.* 86 (1982) 131; (b) K. Iseda, *Bull. Chem. Soc. Jpn.* 64 (1991) 1160.
- [5] M.R. Hoffmann, T.S. Martin, W. Choi, D.W. Bahnemann, *Chem. Rev.* 95 (1995) 69.
- [6] B. Kraeutler, A.J. Bard, *J. Am. Chem. Soc.* 78 (1978) 5985.
- [7] M. Fujihira, Y. Satoh, T. Osa, *Nature* 293 (1981) 206.
- [8] C.-M. Wang, A. Heller, H. Gericher, *J. Am. Chem. Soc.* 114 (1992) 5230.
- [9] (a) W. Kubo, T. Tatsuma, *Anal. Sci.* 20 (2004) 591; (b) W. Kubo, T. Tatsuma, *J. Am. Chem. Soc.* 128 (2006) 16034; (c) T. Tatsuma, S.-I. Tachibana, A. Fujishima, *J. Phys. Chem. B* 105 (2001) 6987.
- [10] T. Hirakawa, K. Yawata, Y. Nosaka, *Appl. Catal. A: Gen.* 325 (2007) 105.
- [11] A.Y. Nosaka, Y. Nosaka, *Bull. Chem. Soc. Jpn.* 78 (2005) 1595.
- [12] J. Schwitzgebel, J.G. Ekerdt, H. Gerischer, A. Heller, *J. Phys. Chem.* 99 (1995) 5633.
- [13] (a) K. Ikeda, H. Sakai, R. Baba, K. Hashimoto, A. Fujishima, *J. Phys. Chem. B* 101 (1997) 2617; (b) K. Ikeda, K. Hashimoto, A. Fujishima, *J. Electroanal. Chem.* 437 (1997) 241.
- [14] (a) V.S. Lisvardi, M.A. Barteau, W.E. Farneth, *J. Catal.* 153 (1995) 41; (b) S.K. Kim, M.A. Barteau, W.E. Farneth, *Langmuir* 4 (1988) 533; (c) Y. Suda, T. Morimoto, M. Nagao, *Langmuir* 3 (1987) 99; (d) I. Carrizosa, G. Munuera, *J. Catal.* 49 (1977) 174; (e) I. Carrizosa, G. Munuera, *J. Catal.* 49 (1977) 189.
- [15] (a) D.S. Muggli, K.H. Lowery, J.L. Falconer, *J. Catal.* 180 (1998) 111; (b) D.S. Muggli, J.T. McCue, J.L. Falconer, *J. Catal.* 173 (1998) 470; (c) D.S. Muggli, S.A. Larson, J.L. Falconer, *J. Phys. Chem.* 100 (1996) 15886; (d) V.S. Lusvardi, M.A. Barteau, W.R. Dolinger, W.E. Farneth, *J. Phys. Chem.* 100 (1996) 18183; (e) D.S. Muggli, J.L. Falconer, *J. Catal.* 175 (1998) 213; (f) S. Pillcentons, S.-J. Hwang, D. Raftery, *J. Phys. Chem. B* 103 (1999) 11152.
- [16] (a) I. Sopyan, M. Watanabe, S. Murasawa, K. Hashimoto, A. Fujishima, *J. Photochem. Photobiol. A: Chem.* 98 (1996) 79; (b) S. Luo, J.L. Falconer, *J. Catal.* 185 (1999) 393.
- [17] (a) E.R. Carraway, A.J. Hoffman, M.R. Hoffman, *Environ. Sci. Technol.* 28 (1994) 786; (b) P.S. Muggli, J.L. Falconer, *J. Catal.* 187 (1999) 230; (c) T. Sakata, T. Kanai, K. Hashimoto, *J. Phys. Chem.* 88 (1984) 2344.
- [18] D.S. Muggli, M.J. Backes, *J. Catal.* 209 (2002) 105.
- [19] (a) J.F. Houlihan, R.J. Pollock, D.P. Madacs, *Electrochim. Acta* 28 (1983) 585; (b) K. Iseda, A. Towata, E. Watanabe, M. Fukuya, H. Taoda, *Bull. Chem. Soc. Jpn.* 71 (1998) 1249; (c) A.V. Vorontsov, V.P. Dubovitskaya, *J. Catal.* 221 (2004) 102; (d) A.V. Vorontsov, E.N. Sainov, G.B. Barannik, V.N. Troitsky, V.N. Parmon, *Catal. Today* 39 (1997) 207.
- [20] (a) W.R. Matthews, *J. Catal.* 111 (1988) 264; (b) J. Schwitzgebel, G.J. Ekerdt, F. Sunada, S.-E. Lindquest, A. Heller, *J. Phys. Chem. B* 101 (1997) 2621; (c) M.M. Kosanic, *J. Photochem. Photobiol. A: Chem.* 119 (1998) 119; (d) L.-F. Liao, W.-C. Wu, C.-Y. Chen, J.-L. Lin, *J. Phys. Chem. B* 105 (2001) 7678; (e) L. Hykrova, J. Jirkovsky, G. Mailhot, M. Bolte, *J. Photochem. Photobiol. A: Chem.* 151 (2002) 181; (f) C. Guillard, P. Theron, P. Pichat, C. Petrier, *Water Res.* 36 (2002) 4263; (g) B.R. Muller, S. Majoni, D. Meissner, R. Mumming, *J. Photochem. Photobiol. A: Chem.* 151 (2002) 253; (h) D.S. Muggli, M.J. Odland, L.R. Schmidt, *J. Catal.* 203 (2001) 51; (i) J.C. Kennedy III, A.K. Datye, *J. Catal.* 179 (1998) 375.
- [21] (a) D.F. Ollis, C.-Y. Hsiao, L. Budiman, C.-L. Lee, *J. Catal.* 88 (1984) 89; (b) J. Chen, D.F. Ollis, W.H. Rulkens, H. Bruning, *Water Res.* 33 (1999) 661; (c) J. Chen, D.F. Ollis, W.H. Rulkens, H. Bruning, *Water Res.* 33 (1999) 669; (d) J. Peral, D.F. Ollis, *J. Catal.* 136 (1992) 554; (e) J.C. Chen, D.F. Ollis, W.H. Rulkens, H. Bruning, *Water Res.* 33 (1999) 1173.
- [22] (a) R.I. Bickley, F.S. Stone, *J. Catal.* 31 (1973) 398; (b) S.A. Larson, J.A. Widegren, J.L. Falconer, *J. Catal.* 157 (1995) 611; (c) D. Brinkley, T. Engel, *J. Phys. Chem. B* 102 (1998) 7596; (d) W. Xu, D. Raftery, *J. Phys. Chem. B* 105 (2001) 4343.
- [23] (a) O.A. Semenikhin, V.E. Kazarinov, L. Jiang, K. Hashimoto, A. Fujishima, *Langmuir* 15 (1999) 3731; (b) B. Ohtani, M. Kakimoto, T. Kagiya, *J. Photochem. Photobiol. A: Chem.* 70 (1993) 265; (c) B. Ohtani, S. Nishimoto, *J. Phys. Chem.* 97 (1993) 920; (d) B. Ohtani, M. Kakimoto, H. Miyadzu, S. Nishimoto, T. Kagiya, *J. Phys. Chem.* 92 (1988) 5773.
- [24] (a) Y. Ohko, K. Hashimoto, A. Fujishima, *J. Phys. Chem. A* 101 (1997) 8057; (b) Y. Ohko, D.A. Tryk, K. Hashimoto, A. Fujishima, *J. Phys. Chem. B* 102 (1998) 2699; (c) Y. Ohko, A. Fujishima, K. Hashimoto, *J. Phys. Chem. B* 102 (1998) 1724.
- [25] (a) A.A. Davydov, M.P. Komarova, V.F. Anufrienko, G.N. Maksimov, *Kinet. Catal.* 14 (1973) 1342; (b) V.V. Nikisha, N.B. Shelimov, B.V. Kazansky, *Kinet. Catal.* 15 (1974) 676; (c) M. Anpo, N. Aikawa, Y. Kubokawa, M. Che, C. Loius, E. Giamello, *J. Phys. Chem.* 89 (1985) 5017; (d) F.R. Howe, M. Gratzel, *J. Phys. Chem.* 91 (1987) 3906; (e) J.M. Coronado, A.J. Maria, J.C. Conesa, K.L. Yeung, V. Augugliaro, J. Soria, *Langmuir* 17 (2001) 5368; (f) C. Murata, H. Yoshida, J. Kumagai, T. Hattori, *J. Phys. Chem. B* 107 (2003) 4364.
- [26] (a) D.C. McCain, W.E. Palke, *J. Magn. Reson.* 20 (1975) 52; (b) R.F. Howe, M. Gratzel, *J. Phys. Chem.* 89 (1985) 4495; (c) M.J. Lopez-Munoz, J. Soria, V. Augugliaro, *Stud. Surf. Sci. Catal.* 82 (1994) 693; (d) X. Li, C. Chen, J. Zhao, *Langmuir* 17 (2001) 4118.
- [27] Y. Nakaoka, Y. Nosaka, *J. Photochem. Photobiol. A: Chem.* 110 (1997) 299.
- [28] L. Xiao-e, A.N.M. Green, S.A. Haque, A. Mills, J.R. Durrant, *J. Photochem. Photobiol. A: Chem.* 162 (2004) 253.

- [29] (a) Y.-C. Kim, K.-H. Lee, S. Sasaki, K. Hashimoto, K. Ikebukuro, I. Karube, *Anal. Chem.* 72 (2000) 3379;  
 (b) Y.-C. Kim, S. Sasaki, K. Yano, K. Ikebukuro, K. Hashimoto, I. Karube, *Anal. Chem.* 74 (2002) 3858;  
 (c) Y.-C. Kim, S. Sasaki, K. Yano, K. Ikebukuro, K. Hashimoto, I. Karube, *Anal. Chim. Acta* 432 (2001) 59.
- [30] (a) C.B. Almquist, P. Biswas, *Chem. Eng. Sci.* 56 (2001) 3421;  
 (b) H. Zhao, D. Jiang, S. Zhang, K. Catteral, R. John, *Anal. Chem.* 76 (2004) 155;  
 (c) L. Zhu, Y. Chen, Y. Wu, X. Li, H. Tang, *Anal. Chim. Acta* 571 (2006) 242.
- [31] T. Hirakawa, T. Daimon, M. Kitazawa, N. Ohguri, C. Koga, N. Negishi, S. Matsuzawa, Y. Nosaka, *J. Photochem. Photobiol. A: Chem.* 190 (2007) 58.
- [32] When the surface organic pollution is photocatalytically decomposed to  $\text{CO}_2$  and  $\text{H}_2\text{O}$ , the large amount of DO is consumed. Hence the surface cleanliness can be estimated by monitoring the DO consumption.
- [33] (a) F. Lipari, S.J. Swarin, *J. Chromatogr.* 247 (1982) 297;  
 (b) J.-O. Levin, K. Amdresson, R. Lindahl, C.-A. Nilsson, *Anal. Chem.* 57 (1985) 1032;  
 (c) K. Mopper, W.L. Stahovec, *Mar. Chem.* 19 (1986) 305.
- [34] (a) J. Schwitzgeble, J.G. Ekerdt, A. Heller, *J. Phys. Chem.* 99 (1995) 5633;  
 (b) J. Schwitzgeble, J.G. Ekerdt, F. Sunada, S.-E. Lindquist, A. Heller, *J. Phys. Chem. B* 101 (1997) 2621;  
 (c) T. Sakata, T. Kawai, K. Hashimoto, *J. Phys. Chem.* 88 (1984) 2344;  
 (d) In our study,  $\text{CH}_3\text{COOH}$  could not be measured. We supposed the reason that the concentration of  $\text{CH}_3\text{COOH}$  that dispersed into bulk solution was too low to be detected by HPLC. In fact, the strong adsorbability of  $\text{CH}_3\text{COOH}$  onto the metal oxide surface as  $\text{TiO}_2$  [34(a)–(c)].
- [35] Generally, the rate of  $\text{I}^{3-}$  formation could distinguish between the  $\text{H}_2\text{O}_2$  and other organic peroxide such as  $\text{R-OOH}$  which is produced by photocatalysis with EtOH because of the different reaction rates. However, in our study, the differences could not be distinguished. Furthermore, the organic peroxide slowly reacts with  $\text{I}^{3-}$  to produce some products and the products might have broad absorption that we observed in this study (the spectra was not shown here). If  $\text{H}_2\text{O}_2$  would be produced at high EtOH concentration region, it would be not higher than  $10\text{ }\mu\text{M}$  based on the results of Fig. 5. The reason is that  $\text{H}_2\text{O}_2$  production is limited by the concentration of DO in closed system in the present study.
- [36] In our study, every experiment was carried out in alkaline condition at pH of 11.5. This condition was intentionally corresponding to previous our work as Ref. [31]. Then the molecular ratio  $\text{HO}_2^-/\text{H}_2\text{O}_2$  is 0.6 in the alkaline solution of pH 11.5.
- [37] M.A. Barakat, J.M. Tseng, C.P. Huang, *Appl. Catal. B: Environ.* 59 (2005) 99.
- [38] (a) C. Kormann, D.W. Bahnemann, M.R. Hoffmann, *Environ. Sci. Technol.* 22 (1988) 798;  
 (b) A.J. Hoffman, E.R. Carraway, M.R. Hoffmann, *Environ. Sci. Technol.* 28 (1994) 776.
- [39] H. Goto, Y. Hanada, T. Ohno, M. Matsumura, *J. Catal.* 225 (2004) 223.
- [40] (a) R. Cai, K. Hashimoto, A. Fujishima, *J. Electroanal. Chem.* 236 (1992) 345;  
 (b) R. Cai, R. Baba, K. Hashimoto, Y. Kubota, A. Fujishima, *J. Electroanal. Chem.* 360 (1993) 237;  
 (c) K. Ishibashi, A. Fujishima, T. Watanabe, K. Hashimoto, *Electrochemistry* 69 (2001) 160.
- [41] R. Nakamura, A. Imanishi, K. Murakoshi, Y. Nakato, *J. Am. Chem. Soc.* 125 (2003) 7443.
- [42] (a) R.-A. Doong, W.-H. Chang, *J. Photochem. Photobiol. A: Chem.* 107 (1997) 239;  
 (b) T.-F. Chen, W.-H. Doong, W.-G. Lei, *Water Sci. Technol.* 37 (1998) 187.
- [43] T. Hirakawa, Y. Nosaka, *Langmuir* 18 (2002) 3247.
- [44] (a) T. Ohno, Y. Masaki, S. Hirayama, M. Matsumura, *J. Catal.* 204 (2001) 163;  
 (b) The precise condition of the peroxide species adsorbed at the  $\text{TiO}_2$  surface is unknown despite several adsorption structure of  $\text{H}_2\text{O}_2$  as peroxide have been suggested [44(a)].
- [45] When  $\text{H}_2\text{O}_2$  is reduced and oxidized to  $\text{H}_2\text{O}$  and  $\text{O}_2$ ,  $\text{TiO}_2$  needs two photons to induce two  $\text{e}^-$  and  $\text{h}^+$  as the reactions (31) and (29).
- [46] (a) D.M. Murphy, E.W. Griffiths, C.C. Rowlands, F.E. Hancock, E. Giamello, *Chem. Commun.* (1997) 2177;  
 (b) J. Yu, J. Chen, C. Li, X. Wang, B. Zhang, H. Ding, *J. Phys. Chem. B* 108 (2004) 2781.
- [47] G.A. Russel, *J. Am. Chem. Soc.* 79 (1957) 3871.